ACS APPLIED MATERIALS & INTERFACES

Research Article

www.acsami.org

Stretchable Polyurethane Sponge Scaffold Strengthened Shear Stiffening Polymer and Its Enhanced Safeguarding Performance

Sheng Wang,[†] Shouhu Xuan,[*,‡] Yunpeng Wang,[‡] Chenhui Xu,[‡] Ya Mao,[†] Mei Liu,[†] Linfeng Bai,[†] Wanquan Jiang,[*,†] and Xinglong Gong[*,‡]

[†]Department of Chemistry, University of Science and Technology of China (USTC), Hefei 230026, P. R. China

[‡]CAS Key Laboratory of Mechanical Behavior and Design of Materials, Department of Modern Mechanics, USTC, Hefei 230027, P. R. China

Supporting Information

ABSTRACT: A simple and scalable "dip and dry" method was developed for fabricating stretchable polyurethane sponge-based polymer composite with excellent shear stiffening effect, creep resisting and adhesion property. The stiffness of the composite was tunable, the storage modulus (G') could automatically increase 3 orders of magnitude with the increasing of shear frequency, and the G'_{max} could reach to as high as 1.55 MPa. Importantly, the composite with ideal damping capacity reduced the impact force by 2 orders of magnitude even under 26 cycles of consecutive dynamic impact loading with no obvious mechanical degradation. Moreover, an enhancing mechanism was proposed and it was found the "B−O cross bond" and the entanglement of polymer chains were attributed to the shear stiffening characteristic. Finally, the excellent adhesion ability and hydrophobicity guarantee the composite with reliable mechanical performance and longer lifespan.

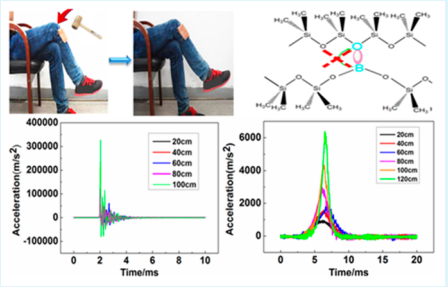

KEYWORDS: *shear stiffening, stretchable polyurethane sponge, adhesion, hydrophobicity, energy dissipation*

1. INTRODUCTION

In the past decades, personal body armor has become a hot research field since terrorism and civil and international conflicts are rising all over the world. Traditional personal body armors are made of rigid materials such as metals[1,2] and ceramics.[3,4] However, the drawbacks of rigidity, inflexibility, and heaviness confined their wide application in the modern eras. Therefore, developing flexible and lightweight body armors is urgent, and so far a series of safeguards based on novel materials have been developed to resist attacks and absorb impact energy.[5−7] One of the most applied flexible materials in energy absorption was polyurethane (PU) sponge, which had the advantages of low density, structural robustness, high porosity, and flexibility.[8−11] So far, flexible and stretchable polymer devices based on sponges have been deeply developed and applied in large numbers of applications, including in environmental protection,[12,13] damping, and energy absorption[14,15]

Shear thickening (ST) is a very common physical phenomenon in many concentrated colloidal suspensions, whose viscosity could be steeply increased once the externally applied shear stress is beyond a critical shear rate and so far much works have been reported by N. Wagner on its rheological properties and mechanisms of ST fluid.[16−18] Owing to the reversible shearing rate activated ST characteristic, shear thickening fluid (STF) is promising to be applied in energy adsorption and body protection to impede severe damages.[19−21] For example, Wagner et al. developed a novel safeguarding composite by embedding SiO_2-based STF into Kevlar fabric and fragment simulation projectile (FSP) ballistic penetration measurements at ∼244 m/s have been conducted to demonstrate the excellent ballistic penetration performance of the composite material.[21] However, shear thickening suspensions are liquid and their unique rheological properties exist within a narrow range of concentration, they are difficult to be used in practical applications. Therefore, several groups introduced the shear thickening fluid into sponge composites with hierarchical macroporous network structures to overcome these disadvantages. Afeshejani et al. studied the energy absorption of neat shear-thickening fluid and the flexible PU sponge soaked in STF.[22] Under impact conditions, the energy absorption of the STF impregnated foam scaffold increased by 85%.[23] Similarly, a smart structure based on commercial foam and shear thickening fluid has been developed and the tunable stiffness characteristics enabled it had potential application in damping.[24] Additionally, Dawson et al. reported the dynamic compressive response of shear thickening fluid-based sponge composite and a mechanical model was proposed.[25]

Since the shear thickening effect occurs in specific condition and the fluid can flow out easily once the STF-based sponge composite is destroyed, its practical application is still limited. To this end, large numbers of attention has been paid to solid

Received: December 11, 2015
Accepted: February 2, 2016
Published: February 2, 2016

DOI: 10.1021/acsami.5b12083
ACS Appl. Mater. Interfaces 2016, 8, 4946−4954

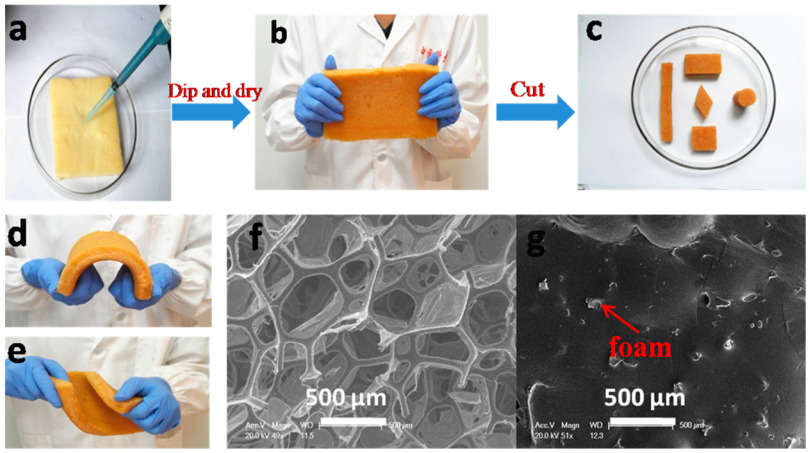

Figure 1. Schematic of the fabrication procedure and the morphologies of the as-prepared samples: preparation pathway (a,b); cut (c), bend (d), and twist (e). SEM images of pristine PU sponge with three-dimensional structures (f) and S-ST/PUC sample (g).

shear-stiffening (S-ST) polymer materials which is a derivative of boron siloxane materials and its modulus can increase with the increasing of external shear force.[26,27] Tian fabricated a novel shear-stiffened elastomer (S-STE) by mixing silicone rubber with silicone oil and investigated the mechanical and rheological properties under both steady-state and dynamic loading conditions.[28] Recently, a novel multifunctional polymer composite with excellent shear stiffening performance and magnetorheological effect was reported and the S-ST properties can be precisely controlled by external triggers.[29] Due to the rate dependent mechanical property and plasticity, shear stiffening (S-ST) polymer has potential application in safeguarding area with polyurethane sponge to resist shock, blast impact, and high strain rate loadings. To this end, polyurethane sponge impregnated with shear stiffening polymer might provide a protective pad with flexibility and high mechanical strength.

In this paper, a stretchable polyurethane sponge (PU) embedded shear stiffening (S-ST) polymer composite was developed by a simple "dip and dry" method. The storage modulus and stress−strain curves of this polymer composite are rate dependent, exhibiting a typical shear stiffening property. The plastic composite is flexible and presents excellent creep resistance. More importantly, this material can dissipate energy efficiently and the impact force is remarkably declined by 2 orders of magnitude. Additionally, the higher specific strength ensures the composite can withstand consecutive dynamic impact loadings with no degradation. A possible mechanism is proposed to analyze the rate dependent mechanical property. Due to the high performance shear-stiffening property, this smart polymer composite is promising to be applied in wearable body armor, vibration controlling, damping, and so forth.

2. EXPERIMENTAL SECTION

2.1. Materials. Acetone and benzoyl peroxide (BPO) were all purchased from Sinopharm Chemical Reagent Co. Ltd., Shanghai, China. Dimethylsiloxane and boric acid were used to prepare shear stiffening polymer, and they were also provided by Sinopharm Chemical Reagent Co. Ltd., Shanghai, China. The above reagents are of analytical purity before use. The 3D-interconnected polyurethane sponge with an apparent core density of 16.56 kg m^{-3} in this work is commercially available.

2.2. Experiments. The polymer matrix in this paper is a derivative of polyborondimethylsiloxane (PBDMS), and the preparation process has been reported in our previous works.[29] A "dip and dry" process is developed to fabricate the polymer composite which is show in Figure 1a,b. First, 100 g of polymer matrix and 4 g of BPO were homogeneously dispersed in 400 mL of acetone solvent in a round-bottomed flask by continuously stirring for 30 min. Second, the suspension was poured into beakers to sonicate for 20 min. Then, the slurry was dropped into the polyurethane sponge and dried under vacuum to remove the acetone. The immersion and drying processes have been repeated for several times until the sponge tended to saturation. Finally, the polyurethane sponges with polymer matrix and BPO were vulcanized in an oven at 50 °C for 2 h. The as-prepared sponges were named as shear stiffening/polyurethane sponge polymer composite (S-ST/PUC).

To improve the hydrophobicity of the S-ST/PUC samples, a multiwalled carbon nanotube based film was coated on the surface. First, the pristine multiwalled carbon nanotube was homogeneously dispersed in 200 mL of a mixed solvent of alcohol and acetone (1/1, v/v) in a round-bottomed flask by stirring continuously for 2 h. Then, the suspensions were pulled into beakers and sonicated. Finally, the slurry was dried under vacuum to remove the solvents. The dried carbon nanotubes were dispersed in acetone. After the preparation, the slurry was dipped on the surface of S-ST/PUC and dried in an oven. Finally, the polymer composite coated by MWCNT was named as M-S-ST/PUC.

2.3. Characterization. The morphology of the PU sponge and S-ST/PUC were characterized by scanning electron microscopy (SEM; JEOL JSM-6700F). The infrared (IR) spectra of PU, S-ST polymer, and the S-ST/PUC were recorded in the full range of 4000−500 cm^{-1} by using a Nicolet model 8700 Fourier transform infrared (FT-IR) spectrometer. Thermal stability of the polymer composite was determined by using a DTG-60H thermogravimetric instrument. The shear stiffening effects of S-ST/PUS specimens were characterized by using a commercial rheometer (Physica MCR 301, Anton Paar Co., Austria). Samples were cut into cylinders with a thickness of 0.68 mm and a diameter of about 20 mm. The shear frequency swept from 0.1 to 100 Hz, and the strain was set at 0.1%. Under the condition of static shear tests, according to strain rate = strain/time, and by changing the sampling time of rheometer, we could obtain the stress−strain curves under the excitation of different rates. Strain increased linearly from 0 to 10% and finally decreased to 0% and by changing the sampling time, the stress−strain loops were obtained. To evaluate the static mechanical property of these materials, the compression strength was tested by using Material Test System (MTS) (MTS criterion 43, MTS System Co., America). Samples were cut into 30 mm × 30 mm × 11 mm pieces and were held by a clamp, and the compression rate was 0.2 mm min^{-1}.

Additionally, a drop hammer test device was applied to study the safeguarding properties of the as-prepared samples. In this process, samples were cut into small pieces with thickness of about 1 cm and

DOI: 10.1021/acsami.5b12083
ACS Appl. Mater. Interfaces 2016, 8, 4946−4954

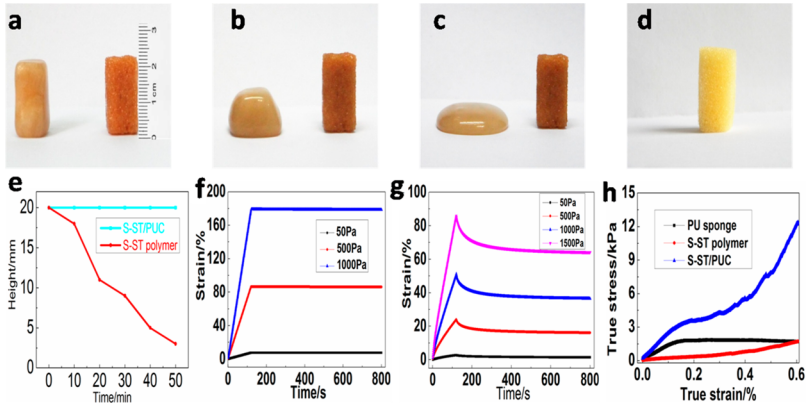

Figure 2. Photographs of the cold flow property of the S-ST polymer matrix and S-ST/PUC sample (a–c); pristine PU sponge (d); height–time curves of the tested samples (e); creep behaviors of the S-ST polymer (f) and S-ST/PUC (g) under different compression stress; static compression stress–strain curves of PU, S-ST polymer, and S-ST/PUC (h).

width by length of 3 × 4 cm^2. During the tests, the drop hammer fell from different heights and the acceleration sensor installed in the drop hammer could record and transform the testing signals into electric signals. The signals passed through the signal-amplifier and finally be recorded and stored in the oscilloscope. Similarly, piercing tests were conducted on the drop hammer test device. A single layer of witness paper was placed on the back of the polymer composite, and the engineered spike (Figure S1, Supporting Information) for 0.625 kg was mounted to the drop mass, fell, and penetrated the witness paper during the tests.

3. RESULTS AND DISCUSSION

After being embedded with S-ST polymer (Figure 1a and b), the as-prepared sample still preserves the mechanical flexibility which can be cut to arbitrary shapes (Figure 1c), bent to any degree (d), and twisted (Figure 1e). When the external force is removed, the polymer composite can return to its original shape without any deformation. Figure 1f and g shows the microstructures of PU sponge and S-ST/PUC sample, respectively. As shown in SEM images, PU sponge has a three-dimensional and cellular-like porous network. The dimension of cellular-like pores is about 500–700 μm which can provide a mechanically stable sponge backbone for S-ST polymer matrix. In Figure 1g, the sponge networks are filled with S-ST polymer and little sponge skeleton can be observed in the surface. Clearly, the polymer is uniformly impregnated into the PU scaffold. It is proved that our "dip and dry" process is effective to prepare a mechanically robust polymer composite with homogeneous dispersion of S-ST polymer matrix in 3D PU sponge.

The FT-IR spectrum of S-ST polymer matrix, PU sponge, and S-ST/PUC sample in the full range of 4000–500 cm^{-1} are tested and shown in Figure S2. Clearly, the FT-IR results of S-ST polymer matrix and S-ST/PUC are quite similar and there is good overlap of these absorption bands since their main components are the same. The characteristic band at 2950 cm^{-1} derives from methyl asymmetric stretching. The absorption peak at 1350 cm^{-1} is ascribed to B–O vibration. The strong absorption band of 1275 cm^{-1} relates to the presence of Si–CH_3 group. The peak of 1100 cm^{-1} indicates the presence of the Si–O bond. A strong absorption band at 890 and 860 cm^{-1} demonstrates the presence of Si–O–B bond. As for PU sponge, the peaks at 3350 cm^{-1} are attributed to the – NH_2 stretching band and 1534 cm^{-1} is its deformation vibration band. A band at 1728 cm^{-1} shows the presence of C═O stretching. These three bands are the characteristic bands of PU. From Figure 1g, PU has no influence on the FT-IR spectrum of S-ST/PUC which is because the content of PU is slight and the infrared (IR) spectrometer cannot detect its signals. Next, the thermal stability of the polymer matrix, PU sponge and S-ST/PUC sample are studied and results are depicted in Figure S2b. The first weight loss of polymer matrix located at 150 °C is due to the evaporation of the adsorbed water and the decomposition of Si-CH_3 structures. The weight loss from 250 to 370 °C is mainly attributed to the decomposition of the organo-silicone structures which includes Si–O, Si–C, and Si–O–B structures. Similarly, the results of polymer matrix and S-ST/PUC are the same and the influence of PU sponge in S-ST/PUC is negligible which are in accordance with the results of FT-IR.

Creep behavior or cold flow property is a common phenomenon in polymer materials which is defined as polymer materials can deform slowly under the excitation of a given constant stress. This phenomenon is time dependent, and the deformation is commonly irreversible. Previously, creep and recovery properties have been investigated to study the viscoelastic mechanisms of polymer materials.[30,31] However, the flow deformation of S-ST polymer is so severe that they have to be sealed so as to keep a definite shape in practical application. As shown in Figure 2a–c, the polymer matrix collapses easily and the height decreases apparently with the increase of time, exhibiting remarkable cold flow characteristic, which will severely restrict its application. Here, the PU sponge can act as a skeleton and the sizes and dimensions of S-ST/PUC are kept constant with the increase of time. Figure 2e is the height versus time curves, the height of S-ST polymer matrix decreases from 20 mm to 3 mm within 50 min while the sizes of S-ST/PUC can keep constant and no creep can be observed. In summary, PU sponge is an ideal supporting material for S-ST polymer matrix and the creep resistance and mechanical property of polymer composite are significantly enhanced.

To further characterize the flow behaviors of S-ST polymer and S-ST/PUC, creep–recovery experiments are carried out under different excitation. Samples are first loaded with a constant stress for about 100 s, then unloaded the stress and samples start to relax. The rheometer records the variations of the sample strain during the test process. Figure 2f and g shows the creep and recovery behaviors of S-ST polymer and S-ST/PUC under different compression stress. Remarkably, strains of

DOI: 10.1021/acsami.5b12083
ACS Appl. Mater. Interfaces 2016, 8, 4946–4954

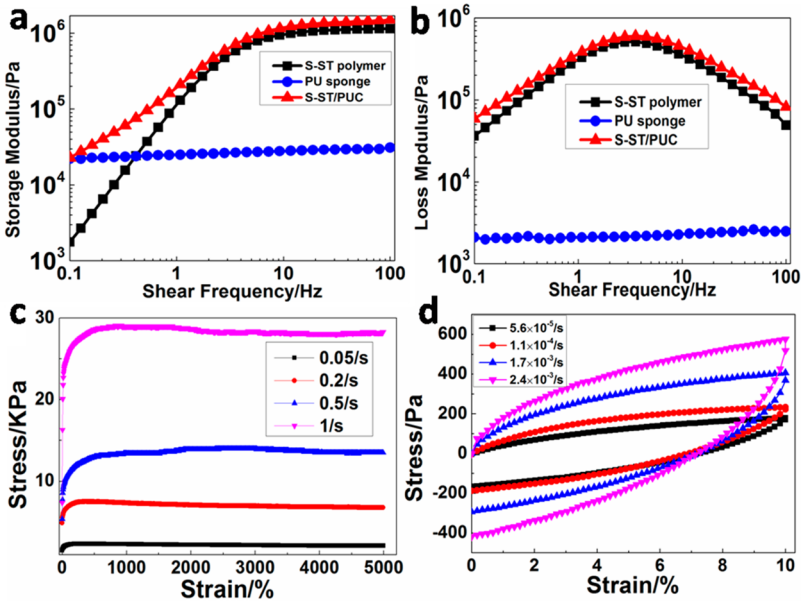

Figure 3. Storage modulus (G') (a) and loss modulus (G'') (b) of S-ST polymer, PU sponge, and S-ST/PUC in the shear frequency tests; stress−strain curves (c) and loops (d) of S-ST/PUC sample under the excitation of different shear rates.

all the samples increase instantaneously once the stress is applied and finally reaches maximum values when getting to the setting creep time and the stress is removed. During the creep stage, strain increases linearly with the increasing of applied stress. However, in comparison to the S-ST polymer, the maximum strain of S-ST/PUC is apparently decreased when they are loaded in the same stress (Figure 2f). For example, the strain of S-ST polymer is 178% on the loading stress of 1000 Pa while the strain of S-ST/PUC is only 51%, which exhibits the creep resistance is obviously improved due to the PU structure. In the recovery periods, the strain of polymer matrix keeps constant with time and no recovery is observed which reveals the strain induced by external stress is viscous flow behavior. However, the S-ST/PUC exhibits viscoelastic properties and a delayed elastic strain decrease to zero which is mainly because of the recovery of PU structures. Additionally, static compression tests were conducted to assess the strength of these materials. As shown in Figure 2h, stresses of all samples are increased with the increasing of strain. Since S-ST polymer is viscoelastic and plastic, it can change the dimension in the direction of static compression force and the stress is lower than PU skeleton. However, the stress of S-ST/PUC is much larger than those of PU sponge and S-ST polymer and the maximum stress is 12.38 kPa which is due to the introduced PU skeleton can significantly enhance the stability and strength of S-ST polymer and it is in accordance with the results before. Based on the above experimental results, we conclude that the S-ST/PUC is viscoelastic and the creep resistance and strength are dramatically improved owing to the introduced PU sponge.

Figure S3 shows the rate-dependent mechanical property of S-ST polymer. The plastic polymer exhibits ductile behavior and fractures abruptly which is due to the shear stiffening effect (b) and can be adhered ideally once the two pieces are contacted with each other (c). Interestingly, the polymer composite can be stretched long enough and be molded into various shapes (d−f). Additionally, the S-ST polymer can be compressed easily by a weight in quasi-static condition (h). However, if impacted violently, shear stiffening effect occurs and the composite can resist the shock dramatically (i). In conclusion, the polymer composite presents typical S-ST mechanical properties with the excitation of external stimuli.

The rheological properties are also investigated to study the rate-dependent mechanical property and the storage modulus (G') and loss modulus (G'') are shown in Figure 3a and b, respectively. Different from other smart materials which often require external power source to be activated, the storage modulus of the tested samples increases obviously with increasing of the shear frequency (Figure 3a). Taking the S-ST polymer, for example, when excited by stress with the shear frequency at 0.1 Hz, its G'_{min} is 1800 Pa, presenting a soft and plastic characteristic. Once the shear frequency reaches to 100 Hz, the G'_{max} increases to 1.02 MPa, which exhibits remarkable shear stiffening property. However, when introduced PU sponge, it dramatically strengthen the mechanical properties of S-ST/PUC. The G'_{min} and G'_{max} are 2.2×10^4 Pa and 1.55 MPa when the shear frequency is 0.1 and 100 Hz, respectively. Figure 3b shows the loss modulus (G'')−shear frequency curves. All the loss moduli of samples increase first and reach to saturation and finally decrease with the increasing of shear frequency. Similarly, the loss modulus of S-ST/PUC is more enhanced than that of S-ST polymer matrix in the same excitation frequency, presenting an enhancement in energy dissipation. As for the PU sponge, the G' and G'' are 2.12×10^4 Pa and 1827 Pa, respectively. With increase of shear frequency, their changes are slight indicating the rheological properties of PU sponge are independent of external stimuli. In this case, it can be concluded that the rate-dependent on rheological properties of S-ST/PUC are mainly attributed to S-ST polymer.

Additionally, the stress−strain curves of S-ST/PUC and PU samples are investigated at various shear rates ranging from 0.05 to 1 s^{-1}. As the shear rate increases, the stress response increase instantaneously, exhibiting representative shear rate dependency (Figure 3c). For example, when excited with the rate at 0.05 s^{-1}, the maximum stress is 2.34 KPa, which presents a plastic characteristic. As soon as the shear rate increases to 1 s^{-1}, the maximum stress reaches to 29.1 KPa, indicating a typical shear stiffening property. In addition, all the stress curves increase with the increasing strain and finally reach to

DOI: 10.1021/acsami.5b12083
ACS Appl. Mater. Interfaces 2016, 8, 4946−4954

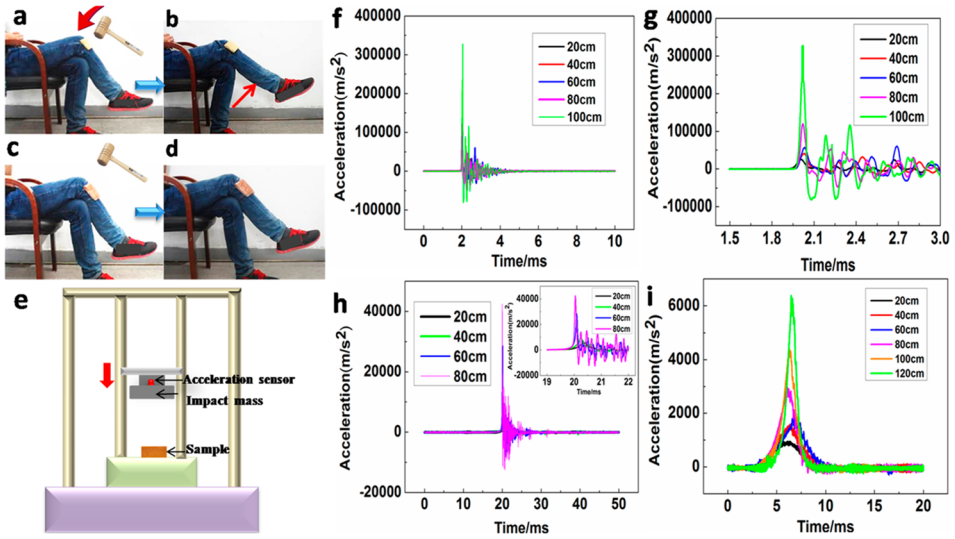

Figure 4. Photographs of energy absorption in knee jerk reflex experiments: (a,b) PU sponge and (c,d) S-ST/PUC composite. (e) Schematic of the drop hammer test devices; the acceleration history of the hammer for (f) no sample; (g) the acceleration peak values of (f); (h) PU sponges and (i) S-ST/PUC samples.

saturation under the excitation of a constant shear rate and no payne effect occurs. Interestingly, during the tests, the as-prepared S-ST/PUC behaved like elastomers and no obvious yield can be observed which is due to the incorporation of PU skeletons. Therefore, the as-prepared composites present a rate dependent characteristic and the modulus and strength can be apparently enhanced once the excitation rate is increased (Figure 3a and c). The stress−strain curves of PU sponge is in Figure S4. In comparison to S-ST/PUC, the changes of stress under the excitation of 0.1, 0.2, and 0.5 s^{-1} are slight and the value is about 36.0 kPa which indicates the strength of PU sample is independent of external shear rates (Figure 3a and b).

In order to further investigate the mechanical properties, especially the damping effects, we systematically conducted the rate dependency of energy dissipation behavior experiments. As displayed in Figure 3d, the area of the stress−strain loop represents the magnitude of energy dissipation. Similarly, the energy dissipation can be greatly enhanced with the increase of shear rates which also demonstrates the energy dissipation performance of S-ST/PUC is rate dependent characteristics. Based on the above results, it is concluded that the S-ST/PUC specimens exhibit remarkable shear stiffening characteristic under the excitation of shear stress with different rates, thus the as-prepared polymer composite can act as a novel kind of flexible protective material.

Due to the shear stiffening effect and rate dependent energy dissipation characteristic, knee jerk reflex experiments are applied to qualitatively illustrate the safeguard performance. In Figure 4a and c, a pure PU sponge and as-prepared S-ST/PUC polymer composite with the length of 10 cm, width of 6 cm, and thickness of 1 cm are placed on the knees and a hammer strikes. In Figure 4b, the PU sponge cannot degrade energy and thus the response of knee jerk reflex is obvious. Particularly, Figure 4d shows the knee nerves cannot sense the significantly reduced impulsive force and no knee jerk reflex is observed. This phenomenon suggests the as-prepared sample can efficiently resist the shock and degrade the impulsive force.

The acceleration signals of drop hammer test are recorded and shown in Figure 4e. During the impact process, the hammer drops from different heights, impacts the tested samples and the acceleration sensor simultaneously captures and transforms the acceleration signals to electric signals. The oscilloscope records the voltage signals and acceleration values (a) could be calculated by $a = kU$, where U is voltage value and the transfer coefficient k is $0.407mV/g$, with g being 10 m/s^2.

Figure 4f is an acceleration−time curve for the case where the hammer strikes on the pedestal of the device. The hammer bounces for several times after impacting and finally damps out. Meanwhile, the acceleration reaches to maximum and the amplitude reduces within 1 ms which is due to the damping characteristics. Figure 4g shows the detailed acceleration amplitude signals of Figure 4f. Dramatically, the peak accelerations (a_{max}) of all amplitudes are increased with the increasing of drop height. For example, a_{max}'s dropping from 80 and 100 cm are, respectively, 120 000 and 330 000 m/s^2, which also indicates the higher the drop height is, the larger the resistance force on the hammer is. Figure 4h and i shows the acceleration−time curves of PU sponges and S-ST/PUC samples, respectively. Compared with the results in Figure 4f, the S-ST/PUC significantly reduces the impact force since the a_{max} is remarkably decreased by 2 orders of magnitude. When the hammer strikes on the S-ST/PUC sample, S-ST effect occurs and the dramatic increase in rate-dependent stiffness can withstand and damp out the impact force and with the increase of drop height, S-ST performance is effective to decrease the force. The a_{max}'s in Figure 4i dropping from 100 and 120 cm are 4200 and 6100 m/s^2, while a_{max} from 100 cm is as high as 330 000 m/s^2 in Figure 4f. Additionally, the interval time of a_{max} in Figure 4i is 10 ms, indicating the viscous-elastic property and buffering effect of S-ST/PUC can absorb and consume the kinetic energy. While in Figure 4f, the interval time is less than 1 ms. As for the pure PU sponge, the waveforms are similar to those in Figure 4f and the improvement in anti-impact ability is not very ideal. In conclusion, the compression rate-dependent stiffness of S-ST/PUC samples are remarkable and the excellent shock resistance significantly reduces the external impact which guarantees its application in safeguards and dampers.

The velocity values are obtained by integrating the acceleration signals, and the initial impact energy E_i can be calculated by $E_i = mgh_0$. The rebound energy E_b is the energy

DOI: 10.1021/acsami.5b12083
ACS Appl. Mater. Interfaces 2016, 8, 4946−4954

which the tested samples can store and release. Figure 5 presents the velocity versus time curves and the relative impact

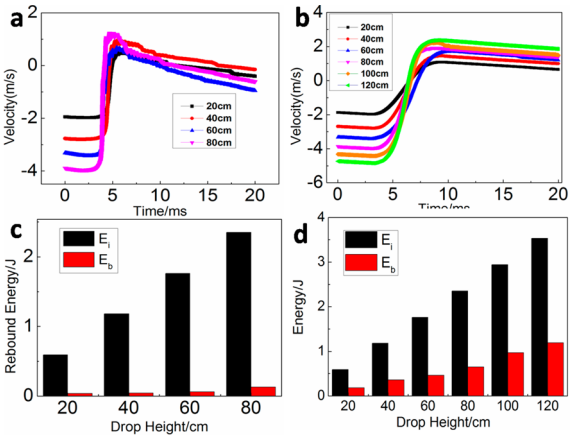

Figure 5. Results of drop hammer experiments: drop hammer velocity versus time impacted on PU sponge (a) and S-ST/PUC composite (b); impact energy and rebound energy (c,d).

energy. Clearly, the velocity is increased with the increasing of drop heights (Figure 5a and b) and E_b in Figure 5d is much higher compared with the results in Figure 5c. Because of the elastic property, the S-ST/PUC can absorb and store much energy (E_b) during the strike. For example, the E_b dropping from 80 cm is 0.72 J. Other parts of impact energy are dissipated by the destruction process of the viscoelastic composite due to its 3D hierarchical structures and excellent energy dissipation properties (according to the results in Figure 3b and d). Therefore, only a small amount of kinetic energy can pass through the polymer composite and absorbed by the pedestal. This is the reason that the a_{max} in Figure 4i is remarkably reduced by 2 orders of magnitude compared with those in Figure 4f and g. As for the PU sponge, the E_b is negligible and most of the impact energy is absorbed by the pedestal of the device, and thus, the a_{max} is much larger. Additionally, the absorbed energy is increasing with the increase of the drop height which indicates the rate-dependent S-ST effect of the polymer composite. Figure S5 shows the piercing test results of PU sponge, S-ST polymer, and S-ST/PUC. Clearly, the PU cannot withstand the impact force of the spike so the witness paper is penetrated seriously. Since S-ST polymer is split and can dissipate energy and resist the spike (Figure S5c), there is only a micropore in the witness paper (Figure S5d). However, as for the S-ST/PUC, there is no pore in the witness paper, which demonstrates it can absorb kinetic energy of the shock and avoid be split effectively. To the end, the S-ST/PUC exhibits excellent energy dissipation and damping properties and is promising to be a novel guarding material for preparing body armors.

To further explore the reliability of cyclic impact on S-ST/PUC sample, we measure its recyclability by using the drop hammer falling from 60 and 100 cm. Figure 6 depicts the repeated rebound energy in cyclic loading process. During the 26 continuous impacts, the rebound energy exhibit fluctuation changes which the E_b^{max} is 0.71 J at the 22nd impact and the E_b^{min} is 0.55 J at 7th loading (Figure 6a). When impacted, part of S-ST/PUC structure is destroyed and the contacts between S-ST polymer matrix and PU sponge are compact, which the shear stiffening effect is more obvious and beneficial for storing energy. This process is attributed to the E_b fluctuation. Since the initial E_b is 0.57 J, it can be concluded that the as-prepared S-ST/PUC sample is highly reliable and no signs of degradation in mechanical strength are appeared even after 26 impact cycles. Figure 6b presents the E_b versus impact cycles from the dropping height of 100 cm. Similarly, E_b increases and shows a slight fluctuation, importantly, retaining its integrity and a relatively stable mechanical performance. In conclusion, the as-prepared S-ST/PUC has excellent and reliable impact-resistance during cyclic loading impacts.

Additionally, the adhesion property of S-ST/PUC is also investigated and demonstrated in Figure 7. An intact S-ST/

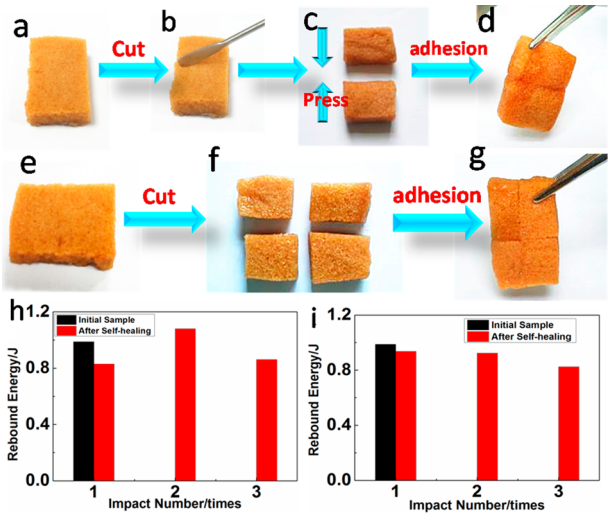

Figure 7. Photographs of the adhesion properties of S-ST/PUC samples. Initial S-ST/PUC samples (a,e) were cut into two (b,c) and four (e,f) pieces; separated pieces were pressed slightly and showed excellent adhesion properties (d,g); the rebound energy (E_b) of the samples before and after adhesion process (h,i).

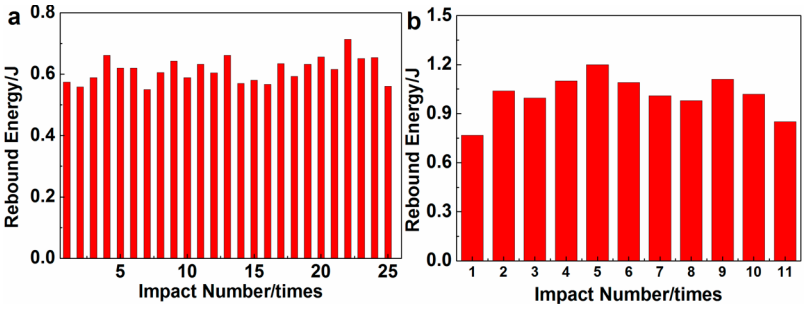

Figure 6. Reliability in rebound energy (E_b) versus cyclic loading impact from 60 cm for 26 times (a) and from 100 cm for 11 times (b).

DOI: 10.1021/acsami.5b12083
ACS Appl. Mater. Interfaces 2016, 8, 4946−4954

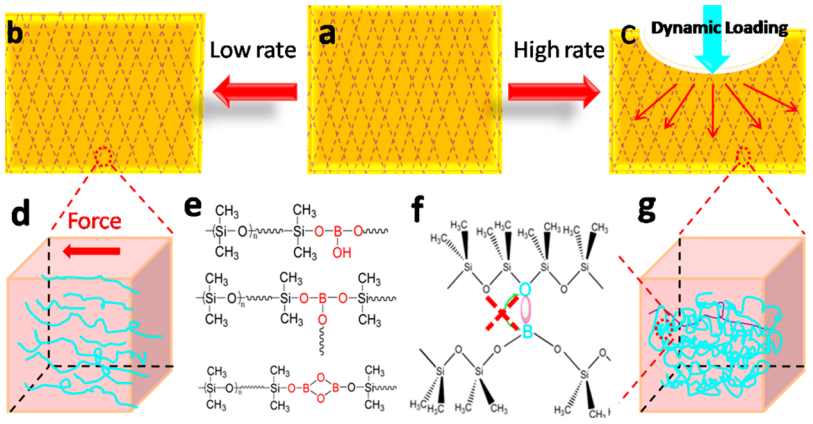

Figure 8. Mechanism of shear stiffening polymer composite with PU sponge: schematic of S-ST/PUC sample (a), chemical formula of S-ST polymer (e); movement of polymer chains if excited with low rate (b,d); shear stiffening effect occurs if excited with high rate (c,g); the "B−O cross bond" (f).

PUC sample is cut into two pieces and the separated pieces are then pressed slightly and can adhere instantaneously. Figure 7d shows the two pieces adhere with each other and the adhesive force can withstand the total weight of sample. Similarly, the other as-prepared S-ST/PUC cut by four pieces also presents excellent adhesion performance (Figure7e−g). Due to the S-ST polymer is viscoelastic in room temperature and the surface is a little sticky, so the viscous S-ST polymer on the skeleton of PU sponge can adhere with each other firmly even the composite is destructed seriously. To further assess the mechanical properties of as-prepared composites before and after healed, the relevant rebound energy under cyclic loading impact are recorded (Figure 7h and i). The average E_b's of Figure 7d and g impacted by 3 times are 0.91 and 0.88 J and the reductions are 4.2% and 7.4% when compared with the initial E_b (0.95 J). Therefore, the healed samples still show ideal impact resistance and the small reduction in E_b over the cyclic loading is possibly due to the slight destruction in the structure of S-ST/PUC. Overall, the as-prepared S-ST/PUC still maintain its structure integrity and stable mechanical performance after adhesion treatment, and the small changes in mechanical properties demonstrate this material can act as reliable body armor even be used after destruction and consecutive impacts, which is beneficial for practical applications. In conclusion, we have successfully proven this novel stretchable soft protective material with excellent adhesion behaviors.

4. MECHANISMS OF RATE-DEPENDENT MECHANICAL PROPERTIES OF S-ST/PUC

Figure 8a shows the formation schematic of the S-ST/PUC. When the boric acid is introduced into dimethylsiloxane, B atoms embed into the polymer chains and form the structures shown in Figure 8e. If S-ST/PUC is excited by external force with low rates, the polymer chains have enough time to relax, disassemble the entanglement and move easily in the direction of the external stress. (Figure 8b and d) In this case, the polymer is flexible and can be molded into various shapes. However, since there are redundant electrons in the orbital of O atoms, they can share electrons with the p-orbital of B atoms and thus forms the "B−O cross bonds". This "cross bond" is transient, dynamically variable and vulnerable than covalent bond which is similar to the hydrogen bond in water. Therefore, if dynamic loaded by the external stress with high rates, the B−O cross bonds cannot break and adjust themselves to adapt to the excitation. Additionally, the massive disordered polymer chains have not enough time to relax and disassemble which will hinder the motion of polymer chains. Under this circumstance, large numbers of the B−O cross bonds can seriously impede the movement of entangled molecular chains. Thus, the storage modulus of the polymer composite is significantly increased and shear stiffening characteristic occurs macroscopically and much energy is dissipated due to the frictions and the movement of polymer chains.

5. SURFACE HYDROPHOBICITY OF S-ST/PUC

Moreover, the surface hydrophobicity is important for improving the resisting corrosion in high humidity conditions. The multiwalled carbon nanotubes (MWCNTs) has been investigated in improving the hydrophobicity of traditional polymer composites in the past decades.[11,32,33] Considering the effectiveness and practicability, we introduced a multiwalled carbon nanotube based film on the surface of the S-ST/PUC to obtain the hydrophobic M-S-ST/PUC. Figure 9a and b shows the SEM images of pristine and the pretreated by organic solvents multiwalled carbon nanotubes. Evidently, there are a large number of bundles in pristine MWCNTs, indicating the conglomeration is very serious which will reduce the

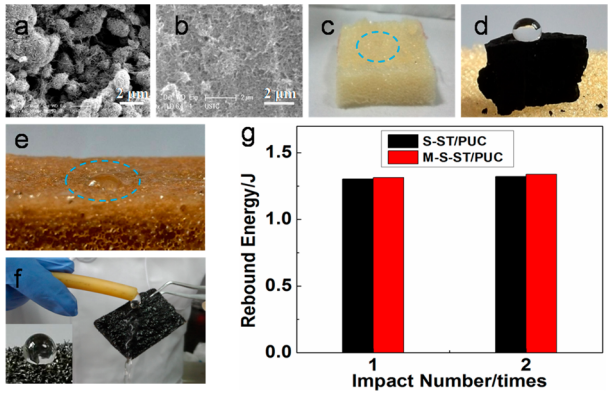

Figure 9. SEM images of pristine (a) and the pretreated by organic solvents multiwalled carbon nanotubes (b); photographs of water on the surface of pristine PU sponge (c), the pretreated multiwalled carbon nanotubes (d), S-ST/PUC sample (e), and M-S-ST/PUC sample (f); E_b of S-ST/PUC sample and M-S-ST/PUC under the impact from 100 cm (g).

DOI: 10.1021/acsami.5b12083
ACS Appl. Mater. Interfaces 2016, 8, 4946−4954

mechanical properties of MWCNTs. However, after the solvent treatment, the dispersion is significant improved and no bundles can be observed in Figure 9b. In conclusion, the excellent dispersity of MWCNTs ensures they can disperse homogeneously in polymer composite.

The wettability of the as-prepared polymer composites is investigated, and the results are shown in Figure 9c–f. As depicted in Figure 9c and e, the water droplet can easily spread on the surface of the PU sponge and S-ST/PUC and be absorbed by them, indicating they are highly hydrophilic However, in contrast to hydrophilic PU sponge and S-ST/PUC, the surface of the pretreated MWCNTs is superhydrophobic and water droplets could easily stand on the surface. Undoubtedly, the MWCNTs deposited on the surface of S-ST/PUC and the water droplet exhibits typical spherical shape on the M-S-ST/PUC, resulting in the transformation of the composite from being hydrophilic to superhydrophilic. (Figure 9f) Additionally, in Figure 9f, water current rapidly flows onto the surface of M-S-ST/PUC. However, the continuous impact force cannot peel off the MWCNTs which reveals the peeling off resistance of coated MWCNTs is large and the prepared composite is stable. This strong adhesion is mainly due to the S-ST polymer is viscoelastic and they can adhere MWCNTs easily. In conclusion, the great water repellency ensures the M-S-ST/PUC can be applied in external conditions even containing much water vapor and prolongs its life span.

Figure 9g shows the E_b of S-ST/PUC sample and M-S-ST/PUC under the impact from 100 cm for twice. Compared with the S-ST/PUC, the E_b of M-S-ST/PUC are almost the same after impacted from 100 cm, indicating that after introducing MWCNT on the surface of S-ST/PUC the mechanical properties remain constant. Above all, the M-S-ST/PUC samples with excellent rate-dependent mechanical properties are also superhydrophobic which guarantees its longer lifespan.

6. CONCLUSION

In this work, a smart and flexible polyurethane sponge with shear stiffening effect, adhesive, and hydrophobic property was prepared by integrating shear stiffening polymer with commercial polyurethane sponge. Rheological tests suggested the mechanical properties, including the storage modulus and stress, were rate-dependent and could response to the environment stimuli automatically. More importantly, the S-ST/PUC composite with shear stiffening property could absorb and dissipate much impact energy and decline the impact force by 2 orders of magnitude. The plastic, flexible, and adhesive characteristics ensured the excellent reliability of the composite under 26 cyclic loading impacts. Additionally, the M-S-ST/PUC with multiwalled carbon nanotubes guaranteed its long life span in wearable body armor, vibration control, damping, and so forth. Finally, the B–O cross bond and the entanglement of polymer chains are believed to be the reason for shear stiffening properties.

■ ASSOCIATED CONTENT

Supporting Information

The Supporting Information is available free of charge on the ACS Publications website at DOI: 10.1021/acsami.5b12083.

Image of engineered spike for piercing tests; FT-IR spectra and TG results; images showing rate-dependent mechanical properties of the S-ST polymer; stress–strain curves PU sponge; schematic of piercing tests of PU sponge (PDF)

■ AUTHOR INFORMATION

Corresponding Authors

*Tel: 86-551-63607605. Fax: 86-551-63600419. E-mail: xusnsh@ustc.edu.cn (S.H.X.).
*E-mail: jiangwq@ustc.edu.cn (W.Q.J.).
*E-mail: gongxl@ustc.edu.cn (X.L.G.).

Notes

The authors declare no competing financial interest.

■ ACKNOWLEDGMENTS

Financial support from the National Natural Science Foundation of China (Grant Nos. 11372301, 11572309, 11572310), Anhui Provincial Natural Science Foundation of China (1408085QA17), and the National Basic Research Program of China (973 Program, Grant No. 2012CB937500) is gratefully acknowledged. This work was also supported by Collaborative Innovation Center of Suzhou Nano Science and Technology.

■ ABBREVIATIONS

ST,shear thickening
STF,shear thickening fluid
S-ST,shear stiffening
PU sponge,polyurethane sponge
S-ST/PUC,shear stiffening/polyurethane sponge polymer composite
MWCNT,multiwalled carbon nanotube
M-S-ST/PUC,mulitwalled carbon nanotube-shear stiffening/polyurethane sponge polymer composite

■ REFERENCES

(1) Karamis, B.; Cerit, A. M.; Nair, F. Mutual Action Between MMCS Structures and Projectile after Ballistic Impact. *J. Compos. Mater.* **2008**, *42*, 2483–2498.
(2) Zhang, G. M.; Batra, R. C.; Zheng, J. Effect of Frame Size, Frame Type, and Clamping Pressure on the Ballistic Performance of Soft Body Armor. *Composites, Part B* **2008**, *39*, 476–489.
(3) Tan, P. Ballistic Protection Performance of Curved Armor Systems without Debondings/Delaminations. *Mater. Eng.* **2014**, *64*, 25–34.
(4) Feli, S.; Asgari, M. R. Finite Element Simulation of Ceramic/Composite Armor under Ballistic Impact. *Composites, Part B* **2011**, *42*, 771–780.
(5) Atanasov, S. E.; Oldham, C. J.; Slusarski, K. A.; Scarff, J. T.; Sherman, S. A.; Senecal, K. J.; Filocamo, S. F.; McAllister, Q. P.; Wetzel, E. D.; Parsons, G. N. Impact Cut-resistance of Kevlar (R) using Controlled Interface Reactions during Atomic Layer Deposition of Ultrathin (< 50 Angstrom) Inorganic Coating. *J. Mater. Chem. A* **2014**, *2*, 17371–17379.
(6) Tan, L. B.; Tse, K. M.; Lee, H. P.; Tan, V. B. C.; Lim, S. P. Performance of an Advanced Combat Helmet with Different Interior Cushioning Systems in Ballistic Impact: Experiments and Finite Element Simulations. *Int. J. Impact. Eng.* **2012**, *50*, 99–112.
(7) Zhou, Y.; Chen, X. G.; Wells, G. Influence of Yarn Gripping on the Ballistic Performance of Woven Fabrics from Ultra-high Molecular Weight Polyethylene Fibre. *Composites, Part B* **2014**, *62*, 198–204.
(8) Yao, H. B.; Ge, J.; Wang, C. F.; Wang, X.; Hu, W.; Zheng, Z. J.; Ni, Y.; Yu, S. H. A Flexible and Highly Pressure-Sensitive Graphene–Polyurethane Sponge Based on Fractured Microstructure Design. *Adv. Mater.* **2013**, *25*, 6692–6698.
(9) Liu, Y.; Ma, J. K.; Wu, T.; Wang, X. R.; Huang, G. B.; Liu, Y.; Qiu, H. X.; Li, Y.; Wang, W.; Gao, J. P. Cost-effective Reduced

DOI: 10.1021/acsami.5b12083
ACS Appl. Mater. Interfaces 2016, 8, 4946–4954

Grapheme Oxide-coated Polyurethane Sponge as a Highly Efficient and Reusable Oli-absorbent. *ACS Appl. Mater. Interfaces* **2013**, *5*, 10018−10026.
(10) Zhang, X. Y.; Li, Z.; Liu, K.; Jiang, L. Bioinspired Multifunctional Foam with Self-Cleaning and Oil/Water Separation. *Adv. Funct. Mater.* **2013**, *23*, 2881−2886.
(11) Engels, H. W.; Pirkl, H. G.; Albers, R.; Albach, R. W.; Krause, J.; Hoffmann, A.; Casselmann, H.; Dormish, J. Polyurethanes: Versatile Materials and Sustainable Problem Solvers for Today's Challenges. *Angew. Chem., Int. Ed.* **2013**, *52*, 9422−9441.
(12) Wu, L.; Li, L. X.; Li, B. C.; Zhang, J. P.; Wang, A. Q. Magnetic, Durable, and Superhydrophobic Polyurethane@Fe_3O_4@SiO_2@Fluoropolymer Sponge for Selective Oil Absorption and Oil/Water Separation. *ACS Appl. Mater. Interfaces* **2015**, *7*, 4936−4946.
(13) Wang, H. Y.; Wang, E. Q.; Liu, Z. J.; Gao, D.; Yuan, R. X.; Sun, L. Y.; Zhu, Y. J. A Novel Carbon Nanotubes Reinforced Superhydrophobic and Superoleophilic Polyurethane Sponge for Selective Oil−Water Separation Through a Chemical Fabrication. *J. Mater. Chem. A* **2015**, *3*, 266−273.
(14) Ge, L.; Xuan, S. H.; Liao, G. J.; Yin, T. T.; Gong, X. L. Stretchable Polyurethane Sponge Reinforced Magnetorheological Material with Enhanced Mechanical Properties. *Smart Mater. Struct.* **2015**, *24*, 037001−037009.
(15) Verdejo, R.; Stampfli, R.; Alvarez-Lainez, M.; Mourad, S.; Rodriguez-Perez, M. A.; Bruhwiler, P. A.; Shaffer, M. Enhanced Acoustic Damping in Flexible Polyurethane Foams Filled with Carbon Nanotubes. *Compos. Sci. Technol.* **2009**, *69*, 1564−1569.
(16) Kalman, D. P.; Wagner, N. Microstructure of Shear-Thickening Concentrated Suspensions Determined by Flow-USANS. *Rheol. Acta* **2009**, *48*, 897−908.
(17) Jiang, W. F.; Xuan, S. H.; Gong, X. L. The Role of Shear in the Transition from Continuous Shear Thickening to Discontinuous Shear Thickening. *Appl. Phys. Lett.* **2015**, *106*, 151902−151906.
(18) Cwalina, C. D.; Wagner, N. J. Rheology of non-Brownian Particles Suspended in Concentrated Colloidal Dispersions at Low Particle Reynolds Number. *J. Rheol.* **2016**, *60*, 47−59.
(19) Wagner, N. J.; Brady, J. F. Shear Thickening in Colloidal Dispersions. *Phys. Today* **2009**, *62*, 27−32.
(20) Zhang, X. Z.; Li, W. H.; Gong, X. L. The Rheology of Shear Thickening Fluid (STF) and the Dynamic Performance of an STF Filled Damper. *Smart Mater. Struct.* **2008**, *17*, 035027.
(21) Lee, Y. S.; Wetzel, E. D.; Wagner, N. J. The Ballistic Impact Characteristics of Kevlar Woven Fabrics Impregnated with a Colloidal Shear Thickening Fluid. *J. Mater. Sci.* **2003**, *38*, 2825−2833.
(22) Afeshejani, S. H.; Sabet, S. A.; Atai, M. E. Energy Absorption in a Shear-Thickening Fluid. *J. Mater. Eng. Perform.* **2014**, *23*, 4289−4297.
(23) Soutrenon, M.; Michaud, V. Impact Properties of Shear Thickening Fluid Impregnated Foams. *Smart Mater. Struct.* **2014**, *23*, 035022.
(24) Soutrenon, M.; Michaud, V. Structural Damping using Encapsulated Shear Thickening Fluids. *Proc. SPIE* **2012**, *8341*, 83410S.
(25) Dawson, M. A.; McKinley, G. H.; Gibson, L. J. The Dynamic Compressive Response of an Open-cell Foam Impregnated with a Non-newtonian Fluid. *J. Appl. Mech.* **2009**, *76*, 061011.
(26) Goertz, M. P.; Zhu, X. Y.; Houston, J. E. Temperature Dependent Relaxation of a "Solid-Liquid". *J. Polym. Sci., Part B: Polym. Phys.* **2009**, *47*, 1285−1290.
(27) Houston, J. E. A Local-probe Analysis of the Rheology of a "Solid liquid". *J. Polym. Sci., Part B: Polym. Phys.* **2005**, *43*, 2993−2999.
(28) Tian, T. F.; Li, W. H.; Ding, J.; Alici, G.; Du, H. P. Study of Shear-stiffened Elastomers. *Smart Mater. Struct.* **2012**, *21*, 125009−125015.
(29) Wang, S.; Jiang, W. Q.; Jiang, W. F.; Ye, F.; Mao, Y.; Xuan, S. H.; Gong, X. L. Multifunctional Polymer Composite with Excellent Shear Stiffening Performance and Magnetorheological Effect. *J. Mater. Chem. C* **2014**, *2*, 7133−7140.
(30) Xu, Y. G.; Gong, X. L.; Xuan, S. H.; Li, X. F.; Qin, L. J.; Jiang, W. Q. Creep and Recovery Behaviors of Magnetorheological Plastomer and its Magnetic-dependent Properties. *Soft Matter* **2012**, *8*, 8483−8492.
(31) Wu, X. Y.; Sallach, R. E.; Caves, J. M.; Conticello, V. P.; Chaikof, E. L. Deformation Responses of a Physically Cross-linked High Molecular Weight Elastin-like Protein Polymer. *Biomacromolecules* **2008**, *9*, 1787−1794.
(32) Wang, C. F.; Lin, S. J. Robust Superhydrophobic/Superoleophilic Sponge for Effective Continuous Absorption and Expulsion of Oil Pollutants from Water. *ACS Appl. Mater. Interfaces* **2013**, *5*, 8861−8864.
(33) Maphutha, S.; Moothi, K.; Meyyappan, M.; Iyuke, S. E. A Carbon Nanotube-infused Polysulfone Membrane with Polyvinyl Alcohol Layer for Treating Oil-containing Waste Water. *Sci. Rep.* **2013**, *3*, 1509−1515.

DOI: 10.1021/acsami.5b12083
ACS Appl. Mater. Interfaces 2016, 8, 4946−4954